

Simple Zinc Complexes of Pyridyl-Substituted Tris(pyrazolyl)borate Ligands

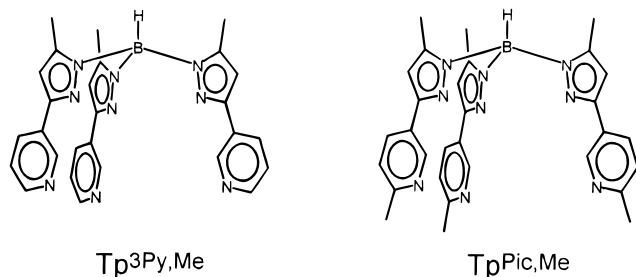
Karl Weis and Heinrich Vahrenkamp*

Institut für Anorganische und Analytische Chemie, Universität Freiburg, Albertstrasse 21, D-79104 Freiburg, Germany

Received May 23, 1997

Treatment of the potassium salts of the Tp^x ligands hydrotris(5-methyl-3-py*-pyrazolyl)borate $\text{Tp}^{3\text{Py},\text{Me}}$ (py* = 3-pyridyl) and $\text{Tp}^{\text{Pic},\text{Me}}$ (py* = 5- α -picolyl) with zinc halides or with $\text{Zn}(\text{ClO}_4)_2$ and KOH yields the halide complexes $\text{Tp}^{3\text{Py},\text{Me}}\text{Zn}-\text{Hal}$ (Hal = F, Cl, Br, I) and the hydroxide complexes $\text{Tp}^{3\text{Py},\text{Me}}\text{Zn}-\text{OH}$ and $\text{Tp}^{\text{Pic},\text{Me}}\text{Zn}-\text{OH}$, as well as the bis(ligand) complex $(\text{Tp}^{3\text{Py},\text{Me}})_2\text{Zn}$. All $\text{Tp}^{3\text{Py},\text{Me}}\text{Zn}-\text{X}$ complexes show a tendency for dimerization, using one pyridyl group each of the two $\text{Tp}^{3\text{Py},\text{Me}}$ units to coordinate to the zinc ion of the opposite $\text{Tp}^{3\text{Py},\text{Me}}\text{Zn}$ fragment, as evidenced by the solid state structures of $\text{Tp}^{3\text{Py},\text{Me}}\text{Zn}-\text{F}$ (strong interaction) and $\text{Tp}^{3\text{Py},\text{Me}}\text{Zn}-\text{I}$ (weak interaction) and by a variable-temperature NMR study of $\text{Tp}^{3\text{Py},\text{Me}}\text{Zn}-\text{OH}$. Despite the steric bulk of the $\text{Tp}^{3\text{Py},\text{Me}}$ ligands, the bis(ligand) complex $(\text{Tp}^{3\text{Py},\text{Me}})_2\text{Zn}$ contains zinc bound to all pyrazole nitrogen donor atoms in an octahedral fashion. $\text{Tp}^{3\text{Py},\text{Me}}\text{Zn}-\text{F}$ crystallizes in the triclinic space group $P\bar{1}$ with $a = 11.123(5)$ Å, $b = 11.638(7)$ Å, $c = 13.793(4)$ Å, $\alpha = 72.34(3)^\circ$, $\beta = 75.32(3)^\circ$, $\gamma = 73.09(5)^\circ$, and $Z = 2$. $\text{Tp}^{3\text{Py},\text{Me}}\text{Zn}-\text{I}$ crystallizes in the monoclinic space group $C2/c$ with $a = 18.922(1)$ Å, $b = 10.476(4)$ Å, $c = 31.444(1)$ Å, $\beta = 101.99(4)^\circ$, and $Z = 8$. $(\text{Tp}^{3\text{Py},\text{Me}})_2\text{Zn}$ crystallizes in the monoclinic space group $C2/c$ with $a = 18.330(2)$ Å, $b = 13.876(1)$ Å, $c = 21.616(1)$ Å, $\beta = 115.96(7)^\circ$, and $Z = 4$.

In the preceding paper,¹ we outlined our interest in tris(pyrazolyl)borate ligands bearing additional donor substituents at the pyrazoles' 3-positions. Our first objects of study in this respect were the 3-pyridyl-substituted Tp^x ligands $\text{Tp}^{3\text{Py},\text{Me}}$ and $\text{Tp}^{\text{Pic},\text{Me}}$. We expected them to combine three properties which



are favorable for allowing and controlling new functionality at the $\text{M}-\text{X}$ unit in $\text{Tp}^x\text{M}-\text{X}$ complexes: (i) sufficient steric bulk to protect the $\text{M}-\text{X}$ function in the Tp^xM pocket; (ii) a favorable polarity due to their donor functions in the vicinity of the $\text{M}-\text{X}$ units, including the ability to become involved in hydrogen bonds; (iii) the ability to attach additional metal ions at the pyridine N atoms and thereby create heterometallic functional entities. $\text{Tp}^{3\text{Py},\text{Me}}$ and $\text{Tp}^{\text{Pic},\text{Me}}$ complement similar Tp^x ligands with 2-pyridyl substituents at the pyrazoles' 3-positions whose pyridine donor functions were found to coordinate to the Tp^x -bound metal itself.²

The structure determinations of the potassium salts of $\text{Tp}^{3\text{Py},\text{Me}}$ and $\text{Tp}^{\text{Pic},\text{Me}}$ ¹ demonstrated that their pyridine N atoms can coordinate to external metal ions, thereby creating molecular dimers or coordination polymers. Our main reason for preparing and studying such ligands is the desire to create a more "natural" environment for zinc ions in complexes modeling zinc enzymes.

We are therefore investigating the full range of the corresponding $\text{Tp}^x\text{Zn}-\text{X}$ complexes. This paper describes the synthesis and structure of the basic $\text{Tp}^x\text{Zn}-\text{X}$ compounds which are to be used as starting materials. Subsequent communications, one of which relating to oligonuclear zinc enzymes has already appeared,³ will deal with the encapsulating ability, the hydrogen-bonding capacity, and the influence on $\text{Zn}-\text{X}$ functionality of the $\text{Tp}^{3\text{Py},\text{Me}}$ and $\text{Tp}^{\text{Pic},\text{Me}}$ ligands.

Experimental Section

The general experimental and measurement techniques were as described previously.⁴ The synthesis of $\text{KTp}^{3\text{Py},\text{Me}}$ and $\text{KTp}^{\text{Pic},\text{Me}}$ was described in the preceding paper.¹ Both were used in the anhydrous form as obtained by pulverization and prolonged pumping.

$\text{Tp}^{3\text{Py},\text{Me}}\text{Zn}-\text{F}$ (1). A solution of $\text{KTp}^{3\text{Py},\text{Me}}$ (500 mg, 0.95 mmol) in methanol/dichloromethane (1:1, 30 mL) was treated successively with $\text{Zn}(\text{ClO}_4)_2 \cdot 6\text{H}_2\text{O}$ (354 mg, 0.95 mmol) and KF (55.3 mg, 0.95 mmol), each in 5 mL of methanol. After 3 h of stirring, the solution was filtered to remove KClO_4 , and the filtrate was evaporated to dryness. Recrystallization from ethanol yielded 402 mg (74%) of 1 as colorless crystals, mp 224 °C. IR (KBr, cm^{-1}): 2552m (BH), 1600w, 1576m, 1543s (ring vibrations). ¹H-NMR (CDCl_3 , δ): 2.58 [s, 9H, Me(pz)], 6.39 [s, 3H, H(pz)], 7.39 [dd, $J = 7.8$ Hz, 4.9 Hz, 3H, py(5)], 8.44 [m, 6H, py(4), py(6)], 8.86 [d, $J = 2.1$ Hz, 3H, py(2)]. ¹⁹F-NMR (CDCl_3 , δ relative CFCl_3): -181.4.

Anal. Calc for $\text{C}_{27}\text{H}_{25}\text{BFN}_9\text{Zn}$ ($M_r = 570.7$): C, 56.82; H, 4.42; N, 22.09. Found: C, 55.66; H, 4.37; N, 21.37.

$\text{Tp}^{3\text{Py},\text{Me}}\text{Zn}-\text{Cl}$ (2). The preparation was analogous to that for 1 with ZnCl_2 (130 mg, 0.95 mmol). Recrystallization from methanol/dichloromethane yielded 497 mg (89%) of 2 as colorless crystals, mp 213 °C. IR (KBr, cm^{-1}): 2556m (BH), 1601w, 1574m, 1542s (ring vibrations). ¹H-NMR (CDCl_3 , δ): 2.58 [s, 9H, Me(pz)], 6.32 [s, 3H, H(pz)], 7.35 [dd, $J = 7.9$ Hz, 4.9 Hz, 3H, py(5)], 8.08 [ddd, $J = 7.9$ Hz, 2.0 Hz, 1.6 Hz, 3H, py(6)], 8.58 [dd, $J = 4.9$ Hz, 1.6 Hz, 3H, py(4)], 8.80 [d, $J = 2.0$ Hz, 3H, py(2)].

Anal. Calc for $\text{C}_{27}\text{H}_{25}\text{BClN}_9\text{Zn} \cdot 1/2\text{CH}_2\text{Cl}_2$ ($M_r = 387.2 + 42.5$): C, 52.45; H, 4.16; N, 20.02. Found: C, 52.97; H, 4.36; N, 20.33.

* Abstract published in *Advance ACS Abstracts*, October 15, 1997.

(1) Weis, K.; Vahrenkamp, H. *Inorg. Chem.* 1997, 36, 5589.

(2) Jones, P. L.; Amoroso, A. J.; Jeffery, J. C.; McCleverty, J. A.; Psillakis, E.; Rees, L. H.; Ward, M. D. *Inorg. Chem.* 1997, 36, 10 and references cited therein.

(3) Ruf, M.; Weis, K.; Vahrenkamp, H. *J. Am. Chem. Soc.* 1996, 118, 9288.

(4) Förster, M.; Burth, R.; Powell, A. K.; Eiche, T.; Vahrenkamp, H. *Chem. Ber.* 1993, 126, 2643.

Table 1. Crystallographic Details

	1	4	7
formula	C ₂₇ H ₂₅ BFN ₉ Zn·C ₂ H ₅ OH	C ₂₇ H ₂₅ BN ₉ Zn·C ₂ H ₅ OH	C ₅₄ H ₅₀ B ₂ N ₁₈ Zn
M _r	616.8	724.7	1038.1
space group	P1̄	C2/c	C2/c
Z	2	8	4
a (Å)	11.123(5)	18.922(1)	18.330(2)
b (Å)	11.638(7)	10.476(4)	13.876(1)
c (Å)	13.793(4)	31.444(1)	21.616(1)
α (deg)	72.34(3)	90	90
β (deg)	75.32(3)	101.99(4)	115.96(7)
γ (deg)	73.09(5)	90	90
V (Å ³)	1600.9(13)	6097.1(5)	4943.2(7)
d _{calc} (g/cm ³)	1.28	1.58	1.40
d _{obs} (g/cm ³)	1.19	1.52	1.41
μ (mm ⁻¹)	0.81	1.86	0.56
R ₁ (obs refl) ^a	0.066	0.034	0.049
wR ₂ (all refl) ^b	0.221	0.102	0.128

$$^a R_1 = \sum |F_o - F_c| / \sum F_o. \quad ^b wR_2 = [\sum w(F_o^2 - F_c^2)^2 / \sum w(F_o^2)^2]^{1/2}.$$

Tp^{3Py,Me}Zn-Br (3). The preparation was analogous to that for **1** with ZnBr₂ (214 mg, 0.95 mmol). Recrystallization from methanol yielded 522 mg (87%) of **3** as colorless crystals, mp 214 °C. IR (KBr, cm⁻¹): 2551m (BH), 1600w, 1572m, 1540s (ring vibrations). ¹H-NMR (CDCl₃, δ): 2.58 [s, 9H, Me(pz)], 6.29 [s, 3H, H(pz)], 7.33 [dd, *J* = 7.9 Hz, 4.9 Hz, 3H, py(5)], 8.03 [ddd, *J* = 7.9 Hz, 2.2 Hz, 1.4 Hz, 3H, py(6)], 8.57 [dd, *J* = 4.9 Hz, 1.4 Hz, 3H, py(4)], 8.78 [d, *J* = 2.2 Hz, 3H, py(2)].

Anal. Calc for C₂₇H₂₅BBN₉Zn (*M_r* = 631.7): C, 51.34; H, 3.99; N, 19.96. Found: C, 50.80; H, 3.99; N, 19.20.

Tp^{3Py,Me}Zn-I (4). The preparation was analogous to that for **1** with ZnI₂ (304 mg, 0.95 mmol). Recrystallization from ethanol yielded 503 mg (78%) of **4** as colorless crystals, mp 216 °C. IR (KBr, cm⁻¹): 2557m (BH), 1600w, 1572m, 1541s (ring vibrations). ¹H-NMR (CDCl₃, δ): 1.23 [t, *J* = 7.0 Hz, 3H, CH₃(ethanol)], 2.59 [s, 9H, Me(pz)], 3.71 [q, *J* = 7.0 Hz, 2H, CH₂(ethanol)], 6.26 [s, 3H, H(pz)], 7.31 [dd, *J* = 7.9 Hz, 4.9 Hz, 3H, py(5)], 7.98 [ddd, *J* = 7.9 Hz, 2.1 Hz, 1.4 Hz, 3H, py(6)], 8.59 [dd, *J* = 4.9 Hz, 1.4 Hz, 3H, py(4)], 8.76 [d, *J* = 2.1 Hz, 3H, py(2)].

Anal. Calc for C₂₇H₂₅BIN₉Zn·C₂H₅OH (*M_r* = 678.7 + 46.1): C, 48.06; H, 4.31; N, 17.40. Found: C, 47.90; H, 4.37; N, 17.18.

Tp^{3Py,Me}Zn-OH (5). A solution of KTp^{3Py,Me} (1.00 g, 1.90 mmol) in methanol/dichloromethane (1:1, 50 mL) was treated successively with Zn(ClO₄)₂·6H₂O (709 mg, 1.90 mmol) and KOH (126 mg, 2.25 mmol), each in 5 mL of methanol. After 3 h of stirring, the solution was filtered, and the filtrate was evaporated to dryness. The residue was taken up in 10 mL of chloroform, the mixture was filtered through a membrane filter, and the filtrate was evaporated to dryness. A 950 mg (88%) quantity of **5** remained as a colorless powder, mp 132 °C, which according to ¹H-NMR was contaminated with ca. 3% **7**. IR (KBr, cm⁻¹): 3546w (OH), 2548m (BH), 1599w, 1574m, 1543s (ring vibrations). ¹H-NMR at 293 K (CDCl₃, δ): 2.58[s, 9H, Me(pz)], 6.32 [s, 3H, H(pz)], 7.34 [very broad, 3H, py(5)], 8.20 [very broad, 3H, py(6)], 8.38 [very broad, 3H, py(4)], 8.81 [broad singlet, 3H, py(2)]. ¹H-NMR data at 223 K are as follows (two sets of resonances for all protons in the intensity ratio 2:1). (i) Set of intensity 2: δ 2.58 [s, 6H, Me(pz)], 6.36 [s, 2H, H(pz)], 7.42 [dd, *J* = 7.7 Hz, 4.0 Hz, 2H, py(5)], 8.21 [d, *J* = 7.7 Hz, 2H, py(6)], 8.51 [d, *J* = 4.0 Hz, 2H, py(4)], 8.85 [s, 2H, py(2)]. (ii) Set of intensity 1: δ 2.61 [s, 3H, Me(pz)], 6.29 [s, 1H, H(pz)], 7.10 [m, 1H, py(5)], 7.62 [m, 1H, py(6)], 7.74 [m, 1H, py(4)], 8.78 [s, 1H, py(2)].

Anal. Calc for C₂₇H₂₆BN₉OZn (*M_r* = 568.8): C, 57.01; H, 4.61; N, 22.17; Zn, 11.50. Found: C, 56.46; H, 4.61; N, 21.46; Zn, 10.96.

Tp^{Pic,Me}Zn-OH (6). The preparation was analogous to that for **5** from KTp^{Pic,Me} (1.00 g, 1.76 mmol), Zn(ClO₄)₂·6H₂O (655 mg, 1.76 mmol), and KOH (116 mg, 2.07 mmol). The residue remaining after evaporation of the chloroform solution to dryness consisted of 910 mg (85%) of **6**, mp 200 °C, containing some cocrystallized solvent which could not be removed by prolonged pumping. IR (KBr, cm⁻¹): 3381m (OH), 2553m, (BH), 1607s, 1570m, 1544m (ring vibrations). ¹H-NMR (223 K, CDCl₃, δ): -0.54 [s, 1H, OH], 2.52 [s, 9H, Me(py)], 2.53 [s,

9H, Me(pz)], 6.29 [s, 3H, H(pz)], 7.28 [d, *J* = 8.4 Hz, 3H, py(5)], 8.07 [dd, *J* = 8.4 Hz, 2.0 Hz, 3H, py(6)], 8.69 [d, *J* = 2.0 Hz, 3H, py(2)].

Anal. Calc for C₃₀H₃₂BN₉OZn·1/2CHCl₃ (*M_r* = 610.9 + 59.7): C, 54.63; H, 4.89; N, 18.80; Zn, 9.75. Found: C, 53.97; H, 5.09; N, 18.88; Zn, 9.84.

(Tp^{3Py,Me})₂Zn (7). A solution of **5** (500 mg, 0.88 mmol) in 10 mL of acetonitrile was heated to reflux for 10 min. After filtration and concentration to 3 mL, the solution was kept at 0 °C to yield 393 mg (86%) of **7** as colorless crystals, mp 175 °C. IR (KBr, cm⁻¹): 2555m (BH), 1572m (ring vibration). ¹H-NMR (CDCl₃, δ): 2.58 [s, 18H, Me(pz)], 5.82 [s, 6H, H(pz)], 6.40 [dd, *J* = 8.0 Hz, 4.3 Hz, 6H, py(5)], 6.77 [d, *J* = 8.0 Hz, 6H, py(6)], 7.76 [s, 6H, py(2)], 8.08 [d, *J* = 8.0 Hz, 6H, py(4)].

Anal. Calc for C₅₄H₅₀B₂N₁₈Zn (*M_r* = 1038.1): C, 62.48; H, 4.85; N, 24.29. Found: C, 61.35; H, 4.73; N, 24.24.

Structure Determinations. Crystals of **1** and **4** were obtained directly from the syntheses as described above; those of **7** were obtained from cyclohexanol/dichloromethane. Diffraction data were recorded at room temperature for **4** and **7** and at 200 K for **1** with the ω/2θ technique on a Nonius CAD4 diffractometer fitted with a molybdenum tube (Kα, λ = 0.7107 Å) and a graphite monochromator. Absorption corrections based on ψ-scans were applied. The structures were solved by direct methods and refined anisotropically with the SHELX program suite.⁵ Hydrogen atoms were included with fixed distances and isotropic temperature factors 1.2 times those of their attached atoms. Drawings were produced with SCHAKAL.⁶ Table 1 lists the crystallographic data.

Results and Discussion

Zinc complexes of (pyrazolyl)borate ligands with bulky substituents were found to be very suitable for reactivity studies of the Zn-X function,⁷⁻¹³ especially in the context of the modeling of zinc enzymes.¹⁴⁻¹⁹ However, while it was shown that the bulk of the substituents have considerable influence on

(5) Sheldrick, G. M. SHELX-86 and SHELXL-93, Programs for Crystal Structure Determination. Universität Göttingen, Germany, 1986 and 1993.

(6) Keller, E. Program SCHAKAL. Universität Freiburg, 1993.

(7) Aisfasser, R.; Powell, A. K.; Trofimenko, S.; Vahrenkamp, H. *Chem. Ber.* **1993**, *126*, 685.

(8) Ruf, M.; Vahrenkamp, H. *Inorg. Chem.* **1996**, *35*, 6571.

(9) Ruf, M.; Schell, F. A.; Walz, R.; Vahrenkamp, H. *Chem. Ber.* **1997**, *130*, 101.

(10) Gorell, I. B.; Looney, A.; Parkin, G. *J. Am. Chem. Soc.* **1990**, *112*, 4068.

(11) Looney, A.; Han, R.; Gorell, I. B.; Corneise, M.; Joon, K.; Parkin, G.; Rheingold, A. L. *Organometallics* **1995**, *14*, 274.

(12) Kläui, W.; Schilde, V.; Schmidt, M. *Inorg. Chem.* **1997**, *36*, 1598.

(13) Darensbourg, D. J.; Holtcamp, M. W.; Khandelwal, K. K.; Klausmeyer, J. H.; Reibenspies, J. H. *Inorg. Chem.* **1995**, *34*, 2389.

the functionality, no system has been investigated yet with other than hydrocarbon substituents. The main reason for this is that pyrazoles with strongly polar substituents do not survive the harsh conditions of the synthesis of the Tp^x ligands. The pyridyl-substituted Tp^x ligands of Ward² and ourselves¹ therefore allow for the first time a study of the influences of ligand polarity and the presence of additional donor functions.

Halide Complexes. The simplest ligand $\text{Tp}^{3\text{Py},\text{Me}}$ was chosen to synthesize all four zinc halide complexes. This posed no problems using the zinc halides, of which zinc fluoride was generated in situ from $\text{Zn}(\text{ClO}_4)_2$ and KF. Complexes **1–4**

$\text{Tp}^{3\text{Py},\text{Me}}\text{Zn}-\text{Hal}$				
No.	1	2	3	4
Hal	F	Cl	Br	I

resulted in very good yields. They could be identified by their IR and ¹H-NMR spectra (see Experimental Section). The positions of the $\nu(\text{BH})$ bands in their IR spectra are 5–30 cm^{-1} higher than those for the corresponding $\text{Tp}^x\text{Zn}-\text{Hal}$ complexes of other Tp^x ligands, thereby giving an indication of a possible polar influence of the pyridyl substituents. The ¹H-NMR spectra of **1–4** point to a symmetrical tridentate coordination by $\text{Tp}^{3\text{Py},\text{Me}}$. The ¹⁹F-NMR resonance of **1** at –181.4 ppm vs CFCl_3 is not very close to those of $(\text{TPMA})\text{Zn}-\text{F}^{20}$ at –125.1 ppm (TPMA = tris((3,5-dimethylpyrazolyl)methyl)amine) and of Kläui's $\text{Tp}^{p-\text{ToI},\text{Me}}\text{Zn}-\text{F}^{12}$ at –219 ppm.

While quite a number of $\text{Tp}^x\text{Zn}-\text{Hal}$ complexes have been subjected to crystal structure determinations,^{21–23} this has so far been the case only for $\text{Tp}^{p-\text{ToI},\text{Me}}\text{Zn}-\text{F}$,¹² and we are not aware of a structure determination of any other zinc–fluoride complex. This prompted us to determine the structure of **1**. After the simplistic information from the ¹H-NMR data, the result was a surprise. Figure 1 shows that **1** forms dimeric molecules in the solid state, the dimerization resulting from the coordination of one pyridyl nitrogen of each $\text{Tp}^{3\text{Py},\text{Me}}$ ligand to the opposing zinc ion. The coordination of the zinc ions is trigonal-bipyramidal to a good approximation; see Table 2. A second pyridyl nitrogen of each $\text{Tp}^{3\text{Py},\text{Me}}$ ligand is involved in a hydrogen bond to a half-occupied ethanol molecule, as is the fluorine atom. A significant part of the force linking the two $\text{Tp}^{3\text{Py},\text{Me}}\text{Zn}-\text{F}$ units seems to come from a stacking interaction between the two aromatic pyridine rings which connect two halves of the dimer across a center of symmetry.

The trigonal-bipyramidal coordination of zinc in a (pyrazolyl)-borate complex is not unprecedented. We have for instance

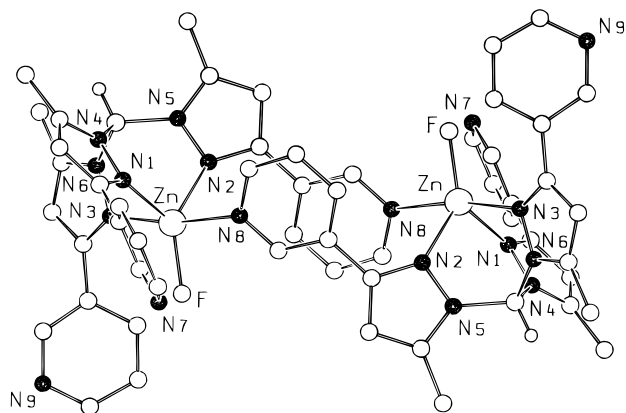


Figure 1. Molecular structure of $\text{Tp}^{3\text{Py},\text{Me}}\text{Zn}-\text{F}$ (**1**).

Table 2. Bond Lengths (Å) and Angles (deg) around the Zinc Ions in $\text{Tp}^{3\text{Py},\text{Me}}\text{Zn}-\text{F}$ (**1**)

Zn–F	1.849(3)	N3–Zn–N8	169.9(1)
Zn–N1	2.041(3)	N3–Zn–F	98.5(1)
Zn–N2	2.056(3)	N3–Zn–N1	87.6(1)
Zn–N3	2.251(3)	N3–Zn–N2	84.0(1)
Zn–N8	2.280(3)	N8–Zn–F	90.2(1)
F–Zn–N1	129.8(1)	N8–Zn–N1	90.8(1)
F–Zn–N2	133.0(1)	N8–Zn–N2	86.3(1)
N1–Zn–N2	97.1(1)		

observed it in $\text{Tp}^{\text{Cum},\text{Me}}\text{Zn}(\text{Cys}-\text{OEt})^{24}$ and in $\text{Tp}^{\text{Cum},\text{Me}}\text{Zn}(\text{cumoylacetate})^{17}$ where the 5-fold coordination of zinc is enforced by the chelating coligands. Complex **1** represents the first case where two monodentate coligands complement the three donor positions occupied by the Tp^x ligand. The linking pattern provided by the two pyridyl groups stacked across a center of symmetry closely resembles that in the potassium complexes of $\text{Tp}^{3\text{Py},\text{Me}}$ (polymeric) and $\text{Tp}^{\text{Pic},\text{Me}}$ (dimeric).¹ The bond distances around the zinc ion are cleanly grouped into three short ones for the equatorial and two long ones for the axial ligands. The Zn–F distance, which is identical to that in $\text{Tp}^{p-\text{ToI},\text{Me}}\text{Zn}-\text{F}^{12}$ but much shorter than the only other reported Zn–F distance in a coordination compound,²⁵ can be compared to the shortest Zn–O distances of Tp^xZn complexes of OH, OR, and RCOO ligands.^{3,7–19}

Having observed the dimerization of **1**, we were interested in discovering whether this is a general phenomenon for all $\text{Tp}^{3\text{Py},\text{Me}}\text{Zn}-\text{Hal}$ complexes or whether the highly electronegative nature of fluorine and hence the enhanced Lewis acidity of zinc make it singular for **1**. For this reason, the structure of the end member of the series, the iodide complex **4**, was determined too. Figure 2 shows that **4**, just like **1**, can be described as composed in the solid state of dimers held together across a center of symmetry by one pyridyl substituent, each being stacked on its equivalent of the opposing $\text{Tp}^{3\text{Py},\text{Me}}\text{Zn}-\text{I}$ unit and weakly coordinating the opposing zinc ion. This similarity includes the hydrogen bonding between the cocrystallized alcohol molecule and one pyridyl nitrogen.

A closer inspection of Figure 2 and of Table 3 reveals, however, that there are significant differences between the structures of **1** and **4**. While the coordination geometry in **1** is trigonal-bipyramidal to a good approximation, that of **4** is better described as a variant of the usual pseudotetrahedral $\text{Tp}^x\text{Zn}-$

(14) Kitajima, N.; Fujisawa, K.; Fujimoto, C.; Moro-Oka, Y.; Hashimoto, S.; Kitagawa, T.; Toriumi, K.; Tatsumi, K.; Nakamura, A. *J. Am. Chem. Soc.* **1992**, *114*, 1277.

(15) Alsfasser, R.; Ruf, M.; Trofimenko, S.; Vahrenkamp, H. *Chem. Ber.* **1993**, *126*, 703.

(16) Ruf, M.; Vahrenkamp, H. *Chem. Ber.* **1996**, *129*, 1025.

(17) Ruf, M.; Weis, K.; Brasack, I.; Vahrenkamp, H. *Inorg. Chim. Acta* **1996**, *250*, 271.

(18) Looney, A.; Han, R.; McNeill, K.; Parkin, G. *J. Am. Chem. Soc.* **1993**, *115*, 4690.

(19) Parkin, G. *Adv. Inorg. Chem.* **1995**, *42*, 291.

(20) Gregorzik, R.; Vahrenkamp, H. Unpublished work.

(21) $\text{Tp}^x\text{Zn}-\text{Cl}$ structures: (a) LeCloux, D. D.; Tolman, W. B. *J. Am. Chem. Soc.* **1993**, *115*, 1153. (b) Yoon, K.; Parkin, G. *J. Am. Chem. Soc.* **1991**, *113*, 8414. (c) Yoon, K.; Parkin, G. *Inorg. Chem.* **1992**, *31*, 1656. (d) Hartmann, F.; Kläui, W.; Kremer-Aach, A.; Mootz, D.; Strerath, A.; Wunderlich, H. *Z. Anorg. Allg. Chem.* **1993**, *619*, 2071.

(22) $\text{Tp}^x\text{Zn}-\text{Br}$ structures: (a) See ref 21b. (b) See ref 21c. (c) Yang, K.; Yin, Y.; Jin, D. *Polyhedron* **1995**, *14*, 1021.

(23) $\text{Tp}^x\text{Zn}-\text{I}$ structures: (a) See ref 21b. (b) See ref 21c. (c) Rheingold, A. L.; White, C. B.; Trofimenko, S. *Inorg. Chem.* **1993**, *32*, 3471. (d) Rheingold, A. L.; Ostrander, R. L.; Haggerty, B. S.; Trofimenko, S. *Inorg. Chem.* **1994**, *33*, 3666.

(24) Ruf, M.; Burth, R.; Weis, K.; Vahrenkamp, H. *Chem. Ber.* **1996**, *129*, 1251.

(25) We found only one compound with a Zn–F interaction in the Cambridge Crystallographic Data File, the polymer $[\text{Zn}(4,4'\text{-bpy})_2]\text{-SiF}_6$ with octahedral zinc and Zn–F distances of 2.08 Å: Subramanian, S.; Zaworotko, M. J. *Angew. Chem.* **1995**, *107*, 2295; *Angew. Chem., Int. Ed. Engl.* **1995**, *34*, 2127.

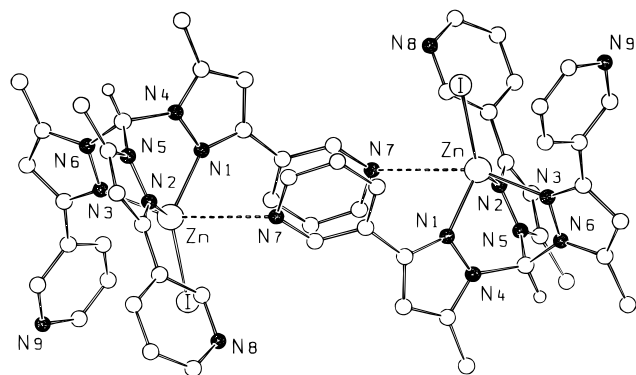


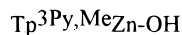
Figure 2. Molecular structure of $\text{Tp}^{3\text{Py,Me}}\text{Zn-I}$ (**4**).

Table 3. Bond Lengths (Å) and Angles (deg) around the Zinc Ions in $\text{Tp}^{3\text{Py,Me}}\text{Zn-I}$ (**4**)

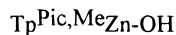
Zn-I	2.5059(4)	N3-Zn-N7	159.1(1)
Zn-N1	2.040(3)	N3-Zn-I	110.9(1)
Zn-N2	2.056(3)	N3-Zn-N1	87.4(1)
Zn-N3	2.122(3)	N3-Zn-N2	91.6(1)
Zn-N7	3.025(3)	N7-Zn-I	88.4(1)
I-Zn-N1	132.23(7)	N7-Zn-N1	73.3(1)
I-Zn-N2	124.92(8)	N7-Zn-N2	83.2(1)
N1-Zn-N2	96.8(1)		

Hal type distorted by the vicinity of a sterically hindering group represented by N7. The Zn-N3 bond is only slightly elongated compared to the Zn-N1 and Zn-N2 bonds, and the Zn-N7 distance is extremely long. If taken as the axial donors of a trigonal bipyramid, N3 and N7 span an angle at zinc (159°) which is far from 180° . The arrangement of the five donor atoms around the zinc ion can be compared to the atomic arrangement in the initial stage of an $\text{S}_{\text{N}}2$ substitution at a tetrahedral center. Obviously the low electronegativity and large size of the iodide ligand render the zinc ion less susceptible to nucleophilic attack, and the stability of the dimer rests to a higher degree on the stacking interaction between the two bridging pyridyl substituents.

Hydroxide Complexes. The modeling of hydrolytic zinc enzymes with Tp^xZn complexes involves the use of the corresponding $\text{Tp}^x\text{Zn-OH}$ species.¹⁴⁻¹⁹ Accordingly, the preparation and use of the Zn-OH complexes of $\text{Tp}^{3\text{Py,Me}}$ and $\text{Tp}^{\text{Pic,Me}}$ were two of the main purposes of the synthesis of these ligands. The Zn-OH complexes **5** and **6** were accessible by our standard



5



6

procedure for the preparation of $\text{Tp}^x\text{Zn-OH}$ compounds,⁸ the reaction of KTP^x with $\text{Zn}(\text{ClO}_4)_2$ and KOH. It turned out, however, that they are not as inert as $\text{Tp}^{t\text{-Bu,Me}}\text{Zn-OH}$,¹⁵ $\text{Tp}^{\text{Ph,Me}}\text{Zn-OH}$,⁹ or $\text{Tp}^{\text{Cum,Me}}\text{Zn-OH}$.⁸ On the one hand, **5** shares the thermal lability of the $\text{Tp}^x\text{Zn-OH}$ complexes without alkyl substituents at the pyrazoles' 5-positions toward dismutation into ZnTp^x_2 and $\text{Zn}(\text{OH})_2$.^{7,15} On the other hand, the amount of KOH used had to be adjusted carefully in order to obtain clean products. When isolated, **5** was always contaminated with small amounts of **7** (see below), and in order to obtain **5** and **6** free from complexes containing H_3O_2^- ligands, a slight excess of KOH had to be used. Using half-molar amounts of KOH resulted in the formation of dinuclear complexes with $\text{Zn}(\mu\text{-H}_3\text{O}_2)\text{Zn}$ units, which may serve as models for oligonuclear zinc enzymes.³

Complexes **5** and **6** could not be obtained as crystals suitable for a structure determination. Their $^1\text{H-NMR}$ spectra at room

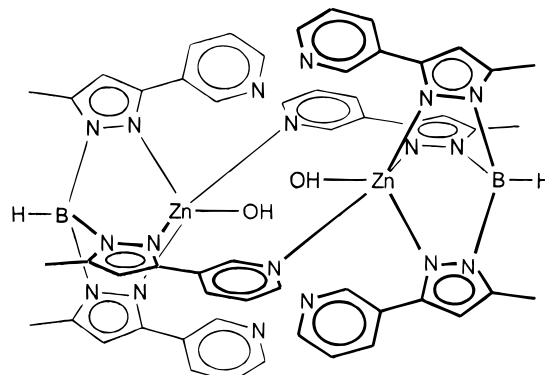


Figure 3. Proposed dimeric structure of $\text{Tp}^{3\text{Py,Me}}\text{Zn-OH}$.

temperature showed the presence of the intact Tp^x ligands but gave no signals for the OH ligands. The latter could be identified by their IR bands. **5** yields a sharp band at 3546 cm^{-1} indicating the presence of an isolated OH group. **6** gives a very broad band at ca. 3380 cm^{-1} whose shape and position point to a hydrogen-bonded situation for the OH group.

In order to obtain more structural information on **5** and **6**, both complexes were subjected to variable-temperature $^1\text{H-NMR}$ measurements (for data, see Experimental Section). For **6**, this yielded little new evidence: there is only one set of sharp resonances for all three pyridylpyrazolyl units at both 293 and 223 K which do not shift upon variation of the temperature. Below 240 K, however, a resonance at -0.54 ppm for the OH group becomes visible in the expected range.¹⁸ From the NMR and IR data, it can be concluded that **6** consists of symmetrical mononuclear $\text{Tp}^x\text{Zn-OH}$ units in solution which at low temperature and in the solid state are weakly linked to neighboring units by $\text{O-H}\cdots\text{O}$ or $\text{O-H}\cdots\text{N}$ hydrogen bonds.

The situation is quite different for **5**. At room temperature, **5** shows broad unstructured $^1\text{H-NMR}$ resonances for the pyridyl 4-, 5-, and 6-protons. Upon cooling, these begin to acquire structure at ca. 260 K. At ca. 250 K, they begin to split, together with all other resonances of the $\text{Tp}^{3\text{Py,Me}}$ ligand. At ca. 220 K, two full sets of fully structured resonances appear which can be assigned to two types of pyridylpyrazolyl groups in an intensity ratio of 2:1. Even at the lowest temperature, no signal for the OH group appears.

The simplest explanation for these observations is a temperature-dependent monomer-dimer equilibrium of **5** in solution. At low temperatures, the association of two monomers occurs via a coordination of one pyridyl nitrogen each to the zinc ion of the second $\text{Tp}^{3\text{Py,Me}}\text{Zn-OH}$ unit. This pairwise interaction (see Figure 3), which is exactly like that observed in the solid state structures of **1** and **4**, differentiates the pyridylpyrazolyl entities into groups of two and one. It is to be expected that the dimeric structure of **5** is also present in the solid state. Conversely, the presence of the methyl groups on the pyridyl substituents in **6** (and probably other $\text{Tp}^{\text{Pic,Me}}\text{Zn-X}$ complexes) seems to be sufficient to prevent this type of dimerization.

The Bis(ligand) Complex ($\text{Tp}^{3\text{Py,Me}}_2\text{Zn}$ (7**)).** Attempts to grow single crystals of **5** led to the accidental structure determination of **7**. This made it clear that **7** is the compound which contaminates **5** and that **5** is labile in solution with respect to the dismutation into **7** and $\text{Zn}(\text{OH})_2$. Subsequently, it was verified that the thermal decomposition of **5** is the method of choice for an almost quantitative formation of **7**.

Complex **7** complements the series of ZnTp^x_2 complexes whose structures have been determined.^{11,21d} The zinc ion in **7** is located on a 2-fold axis, and the relation between the two $\text{Tp}^{3\text{Py,Me}}$ ligands is that of a 2-fold rotation. Figure 4 and Table

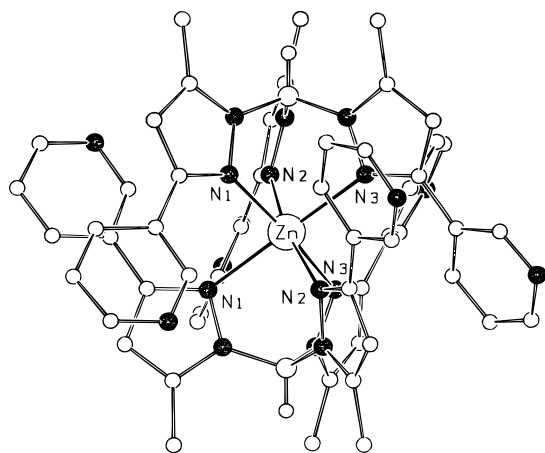


Figure 4. Molecular structure of $(\text{Tp}^{3\text{Py,Me}})_2\text{Zn}$ (**7**).

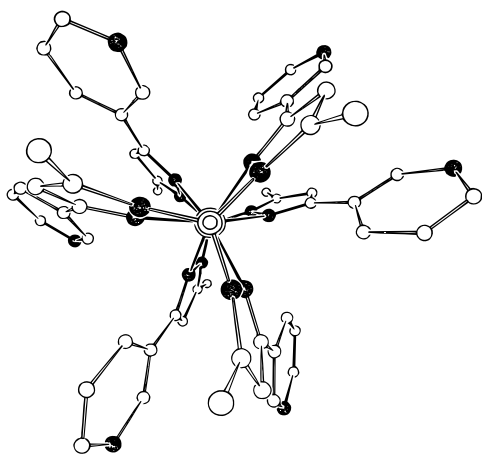


Figure 5. Perspective view of **7** along its 3-fold axis.

Table 4. Bond Lengths (Å) and Angles (deg) around the Zinc Ion in $(\text{Tp}^{3\text{Py,Me}})_2\text{Zn}$ (**7**)

Zn–N1	2.226(4)	N1–Zn–N2	87.5(1)
Zn–N2	2.227(3)	N1–Zn–N3	88.3(1)
Zn–N3	2.265(4)	N2–Zn–N3	87.5(1)
N1–Zn–N3'	170.6(1)	N1–Zn–N1'	86.4(2)
N2–Zn–N2'	169.9(2)	N1–Zn–N2'	99.9(1)
N3–Zn–N1'	170.6(1)	N2–Zn–N3'	85.9(1)
		N3–Zn–N3'	98.0(2)

4 illustrate the distorted octahedral coordination of the zinc ion which is typical for ZnTp^x_2 complexes.¹⁴ Figure 5 shows how the six pyridylpyrazolyl groups are intertwined in a propeller-like fashion.

The formation and structure of **7** came as a surprise. On the basis of our experience with Tp^x ligands with methyl substituents on the pyrazoles' 5-positions and bulky substituents on the pyrazoles' 3-positions, we would have expected the $\text{Tp}^x\text{Zn}-\text{OH}$ complex **5** to be stable toward a thermal dismutation.^{8,15} Furthermore the Tp^{Ph} ligand, whose phenyl group on the 3-position has exactly the same steric requirements as the pyridyl group on the 3-position in $\text{Tp}^{3\text{Py,Me}}$, forms a ZnTp^x_2 complex containing tetrahedral zinc coordinated by only two pyrazolyl nitrogens of each Tp^{Ph} .²⁵ On the other hand, Figure 5 shows that there is room for the intertwining of the six pyridylmethyl units. Figure 5 also shows that there is a weak stacking interaction for each pyridyl ring with a pyrazolyl ring of the opposing $\text{Tp}^{3\text{Py,Me}}$ ligand. This interaction finds its expression in the ¹H-NMR resonances of the pyridyl substituents which are shifted upfield for almost 1 ppm in comparison to those of **1** or **5**. Finally, it is worth mentioning that the pyridyl nitrogen atoms in **7** show no interactions whatsoever with zinc ions.

Conclusions

The two new ligands which are easily accessible have been shown to yield a zinc complex chemistry which promises new structural and reactivity patterns. The complex types $\text{Tp}^x\text{Zn}-\text{Hal}$ and $\text{Tp}^x\text{Zn}-\text{OH}$, which will serve as starting materials for a derivative chemistry, can be obtained in very good yields. Their structure determinations have confirmed that the new qualities of the ligands—ability to coordinate external metal ions and ability to become involved in hydrogen bonds—are operational. All three structure determinations have revealed furthermore that stacking interactions between the heteroaromatic rings provide significant contributions to structural stability. The two $\text{Tp}^x\text{Zn}-\text{OH}$ compounds are the first in Tp^xZn chemistry with polar groups in the pocket surrounding the Zn–OH reaction center. Further papers in this series will describe how this affects the biomimetic chemistry of the Zn–OH function and how the different solution behaviors of $\text{Tp}^{3\text{Py,Me}}\text{Zn}-\text{OH}$ and $\text{Tp}^{\text{Pic,Me}}\text{Zn}-\text{OH}$ find expression therein.

Acknowledgment. This work was supported by the Deutsche Forschungsgemeinschaft and by the Fonds der Chemischen Industrie. We thank Mr. B. Müller and Dr. W. Deck for measurements and data collection.

Supporting Information Available: Fully labeled ORTEP plots for all three structures (3 pages). Three X-ray crystallographic files, in CIF format, are available on the Internet only. Ordering and access information is given on any current masthead page.

IC970628J